Dissipative Acid-Fueled Reprogrammable Supramolecular Materials

Enzo Olivieri, Baptiste Gasch, Guilhem Quintard, Jean-Valère Naubron, Adrien Quintard

Dissipative Acid-Fueled Reprogrammable Supramolecular Materials

Enzo Olivieri, Baptiste Gasch, Guilhem Quintard, Jean-Valère Naubron, and Adrien Quintard*

ABSTRACT: Smart materials reversibly changing properties in response to a stimuli are promising for a broad array of applications. In this article, we report the use of trichloroacetic acid (TCA) as fuel to create new types of time-controlled materials switching reversibly from a gel to a solution (gel−sol−gel cycle). Applying various neutral amines as organogelators, TCA addition induces amine protonation, switching the system to a solution, while TCA decarboxylation over time enables a return to the initial gel state. Consequently, the newly obtained materials possess interesting time-dependent properties applied in the generation of remoldable objects, as an erasing ink, as chiroptical switches, or for the generation of new types of electrical systems.

KEYWORDS: organogel, smart material, dissipative assembly, supramolecular, chirality
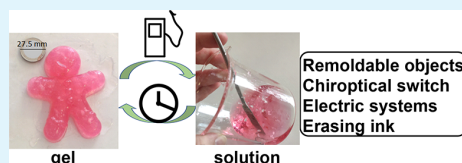
INTRODUCTION

Mimicking nature's formidable tools at work in many biological processes, the field of chemically fueled out-of-equilibrium systems has recently started gaining attention.[1] A time-dependent switch of a chemical, physical, or biological property can be obtained upon the addition of fuel. This has notably been applied to trigger changes in supramolecular assemblies such as gelation−degelation phenomena.[2−8] It has a great potential for future applications as smart materials, switching with temporal control between different states.[8,9] However, despite the tremendous progress achieved in the last years, this field is still in its infancy, and considerable progress is required before its implementation to real-life applications.[10−18] For example, many systems rely on complex enzymatic settings for success,[5] cannot be reproduced upon multiple cycles, or lack robustness. For this field to come to maturity, it is mandatory to uncover reliable systems based on simple chemicals and possessing applicable properties.
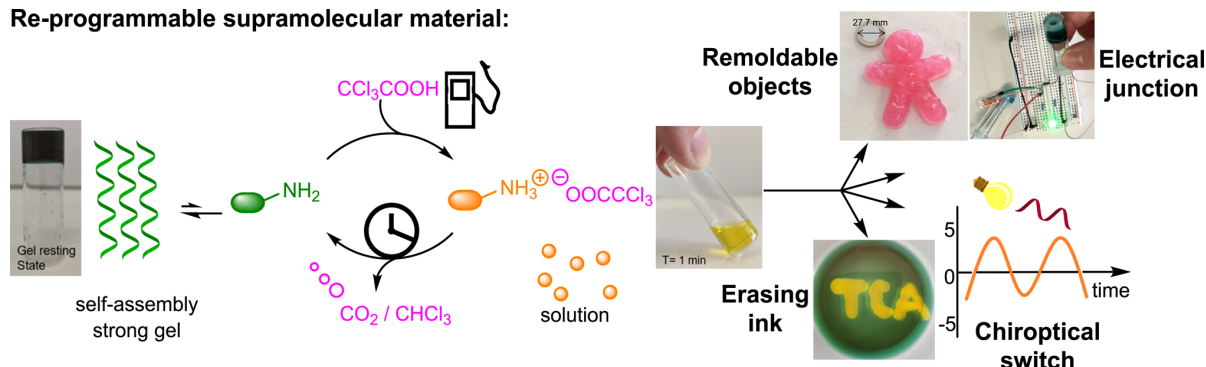
In the literature, most dissipative systems have focused on the temporary gelation of a solution upon the addition of a fuel (sol−gel−sol transition),[2−29] and only limited examples of the complementary temporary degelation (gel−sol−gel transition) have been reported.[30−39] To build an easily available and reliable system for gel−sol−gel transition, we focused on the application of trichloroacetic acid (TCA) as chemical fuel. This cheap acid has been applied with success in the elaboration of different out-of-equilibrium molecular switches.[40−52] It enables the temporary protonation of amines, leading back to the free amines upon volatile CO_2 and chloroform liberation, which avoids any potentially problematic waste accumulation. In the presence of an additional strong base such as DBU, additional complexity is observed through a three-state switch of the amine between the protonated, neutral, and anionic state through carbamate formation.[53]

To create a convenient and practical approach toward temporary degelation, herein, we disclose complementary gel−sol−gel systems based on the temporary protonation of different primary amines upon TCA addition (Figure 1). From a self-assembling neutral amine (gel), the addition of a strong acid (TCA) drives the system out of equilibrium to the temporary protonated amine solution. Amine-catalyzed TCA decarboxylation displaces the system over time back again to the neutral amine and to the resulting self-assembly (strong gel). The system involves simple-to-use and widely available components and, upon fuel consumption, releases non-accumulating volatile CO_2 and chloroform, thus ensuring the good operability of the system over multiple cycles. This approach is general for different self-assembling amines, providing materials with complementary properties. The interest of the materials developed was demonstrated in diverse applications ranging from remoldable objects, chiroptical switches, and erasing inks to reusable flexible electric junctions with temporal control, demonstrating the potential of these materials.
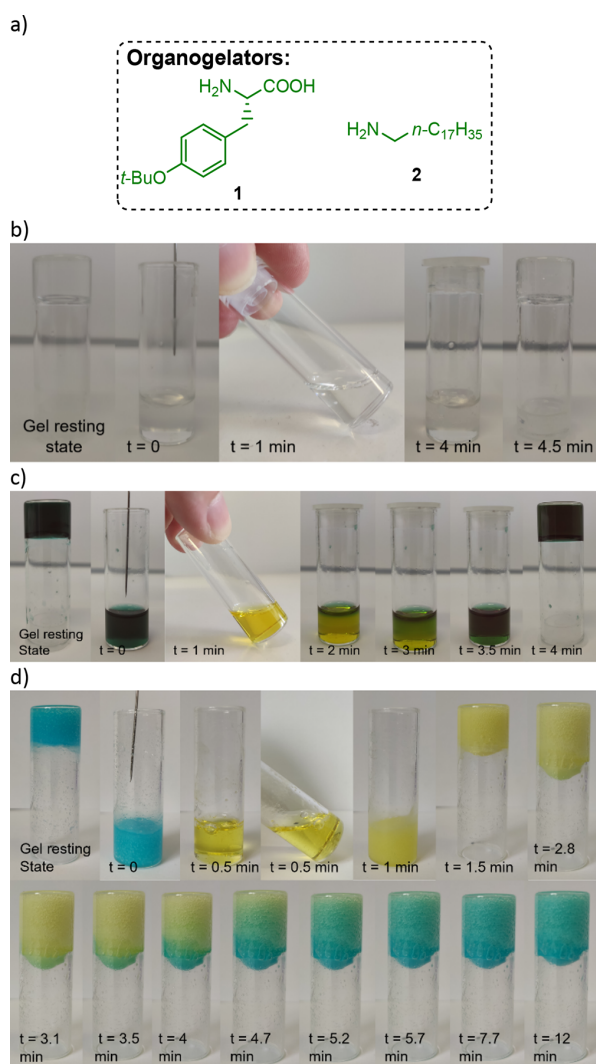
RESULTS AND DISCUSSION

At first, to prove the feasibility of a TCA-fueled gel−sol−gel transition, we focused on the use of simple and cheap gelating amines, O-tert-butyl-L-tyrosine **1**[54] and octadecylamine **2**,[55,56] using DMF or DMSO as solvent (Figure 2). Gratifyingly, from the neutral gels, the addition of excess TCA did induce the

Figure 1. CCl$_3$COOH fueled time-programmable functional material.

a)

Organogelators:

1

2

b)

Gel resting state — t = 0 — t = 1 min — t = 4 min — t = 4.5 min

c)

Gel resting State — t = 0 — t = 1 min — t = 2 min — t = 3 min — t = 3.5 min — t = 4 min

d)

Gel resting State — t = 0 — t = 0.5 min — t = 0.5 min — t = 1 min — t = 1.5 min — t = 2.8 min

t = 3.1 min — t = 3.5 min — t = 4 min — t = 4.7 min — t = 5.2 min — t = 5.7 min — t = 7.7 min — t = 12 min

Figure 2. (a) Organogelators used in this study. (b) TCA (0.159 mmol) fueled a gel−sol−gel process using **1** (0.0420 mmol) in 1 mL of DMF. (c) TCA (0.159 mmol) fueled a gel−sol−gel process using **1** (0.0420 mmol) in 1 mL of the DMF/BTB/BPB solution. (d) TCA (0.196 mmol) fueled a gel−sol−gel process using **2** (0.148 mmol) in 1 mL of the DMSO/BTB solution.

desired formation of a clear solution in a few seconds followed by the return to the initial gel state after 3 to 5 min (see Supporting Information (SI) for conditions). For example, using O-tert-butyl-L-tyrosine **1** in DMF (1 wt/v %), pictures monitoring the gel−sol−gel process are given in Figure 2b. It must be pointed out that gelation was not limited to DMF but was also efficient using solvents such as acetonitrile, acetone, ethyl acetate, benzene, or dichloromethane (Table S1). When modulating the solvent, since the rate of decarboxylation is strongly solvent-dependent, the time to gelation ranged from a few minutes to several days, increasing the tunability of the systems.

To better visualize the gel−sol−gel transition and monitor TCA consumption, a tiny amount of bromothymol blue (BTB) and bromophenol blue (BPB), two acid-sensitive indicators, was added to the system. This enables a clear visualization of the dissipative system evolving from the initial green-blue gel to the protonated yellow solution and back again to a green-blue gel as soon as enough neutral amine is formed. While for O-tert-butyl-L-tyrosine **1** in DMF (Figure 2b,c) the gelation provides a strong and compact gel, using octadecylamine **2** in DMSO (4 wt/v %) unlocks access to gels with totally different aspect (Figure 2d, see SI for gels generated without colored additives). Indeed, a much weaker gel entrapping CO$_2$ bubbles is formed upon TCA decarboxylation. Thanks to the use of DMSO as solvent, the decarboxylation is much faster. It provides after 1.5 min a sufficient concentration of the gelator to start the gelation, while all the ammonium ions are not fully decarboxylated as can be seen from the remaining yellow color coming from the acid-sensitive indicator (BTB).

The rheological properties of the system were also studied over two successive TCA additions (Figures S6, S7, and S12). This confirmed that TCA addition generated a solution evolving back to the gel upon TCA decarboxylation and formation of the neutral amines. These experiments also confirmed the difference in gel strengths observed using the two amines. At 0.46 wt/vol % of amino acid **1**, a strong gel was formed highlighted by the high storage modulus (G′) (10,000 Pa) and loss modulus (G″) (3000 Pa). In sharp contrast, the gel formed using 4 wt/vol % of linear amine **2** was by far less elastic and viscous, providing a G′ of 500 Pa and a G″ of 250 Pa. With these two amines, upon the second TCA addition, solutions of low G′ and G″ are generated again, evolving back again to the same gels upon time-dependent TCA decarboxylation.

Importantly, the time of the temporary event can be controlled efficiently through the chemical fuel concentration. The TCA-dependent kinetics of gelation could be confirmed using **1** through the monitoring of light dispersion absorbance at 400 nm (Figure 3a; see Figure S11 for results with **2**).
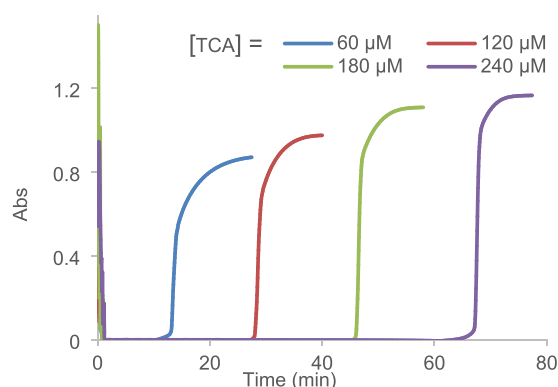
Figure 3. [TCA] time dependence of the gel−sol−gel system as monitored through UV absorption at 400 nm. **1** (0.021 mM) in DMF.

Indeed, from a slightly turbid gel, TCA addition induces the formation of a clear solution before going back to the initial gel. Increasing the [TCA] concentration from 60 to 240 μM delayed the return to a gel from 14 to 68 min. From these curves, the time between the onset of absorbance increase and equilibrium decreases with the increasing amount of fuel (from 60 to 240 μM). This might be indicative of a slight modification of the system through higher concentrations in CO_2 and chloroform upon TCA decarboxylation impacting the rate of nucleation. It must be pointed out that the rate of nucleation is also dependent on the volume of the solution (Figures S6 and S7).

Interestingly, the gel−sol−gel process using *O-tert*-butyl-L-tyrosine **1** in DMF could also be applied to obtain a chiroptical switching material of great potential for the development of logic gate devices or data storage (Figure 4).[57−62] During the gel−sol−gel cycles, from the negative gel signals, TCA additions induce a fast response of the system within a few seconds, providing positive electronic circular dichroism (ECD) signals of equal intensity. This is followed by a positive plateau during which excess TCA is present. As soon as most TCA has been removed through decarboxylation, the signal slowly starts to decrease until a critical concentration in neutral amino acid is obtained (see Figure S8 for enlarged spectra). This triggers a rapid nucleation with a fast decrease in the ECD signal to reach the negative plateau corresponding to the gel resting state. Monitoring of the gel−sol−gel cycles with linear dichroism spectroscopy shows that gel formation is accompanied by the occurrence of a non-negligible LD signal (Figure S9). This LD signal, whose intensity remains almost constant over the cycles, highlights an orientation of the fibers that compose the gel. In contrast to ECD, the UV absorbance increases strongly within the first two cycles before gradually stabilizing over the following cycles. This behavior, similar to the one observed when monitoring the dispersion at 400 nm during the cycles (Figure 3), is probably related to an increase of the dispersive properties of the gel through a saturation in CO_2.
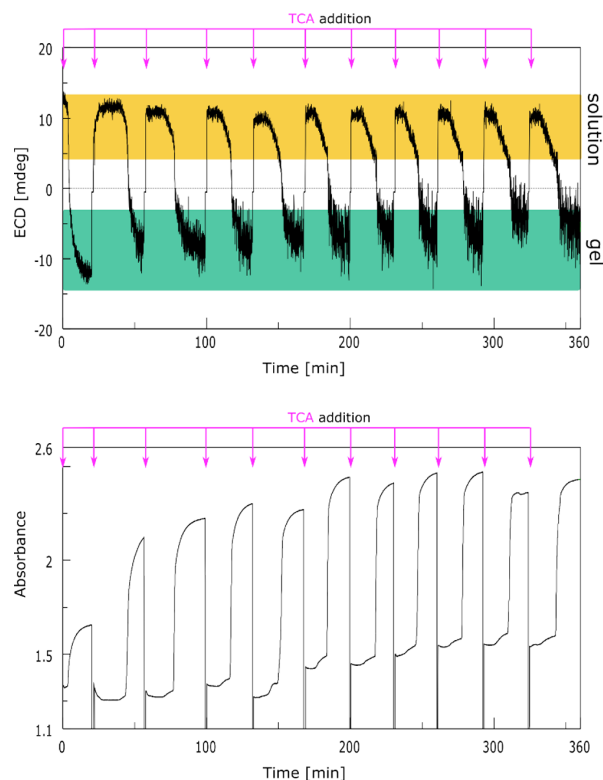
Figure 4. Time course of ECD at 279 nm over multiple gel−sol−gel cycles upon successive TCA additions. **1** (0.021 mM) in DMF at 20 °C. Successive additions of TCA (0.06 mM). ECD signal: green = gel; yellow = solution.

Demonstrating the reliability of the system, upon successive TCA additions, the gel−sol−gel transition could reliably be repeated over at least 15 cycles (Figure 4). Of interest, the different signals are stable and not impacted by the multiplication of the gel−sol−gel cycles.

The strong resistance of the gel obtained and the simplicity and reliability of the system coupled with the availability of both gelators and fuel make it attractive for applications as functional materials. At first, the gel−sol−gel transition was used to generate remoldable objects (Figure 5a).[8,9] For this purpose, using **1** as gelator, a 60 mL DMF gel was generated in a vial. Adding TCA, a solution was formed and transferred to a mold, affording after 5 min a man-figure gel resistant enough to be handled. This process could be repeated again to generate successively two "candy canes" and a new man-type gel through TCA-fueled gel−sol−gel transitions (see also Figures S18−S21). This demonstrates the ability of the TCA system to remold objects under mild conditions. Aside from remoldable objects, the gel−sol−gel ability in combination with the addition of acid-sensitive colored additives could be applied to generate disappearing messages on the gel through the use of TCA as a disappearing ink (Figure 5b).[12,30,34] This strategy is of interest in the context of the application of alternative cryptography systems that is mandatory to discover new approaches to encrypt secret information. From the acid colored indicator doped green strong gel matrix, the word TCA was written by the addition of a solution of TCA. At the contact with the TCA solution, the gel dissolved and became yellow, while the rest of the gel structure remained untouched
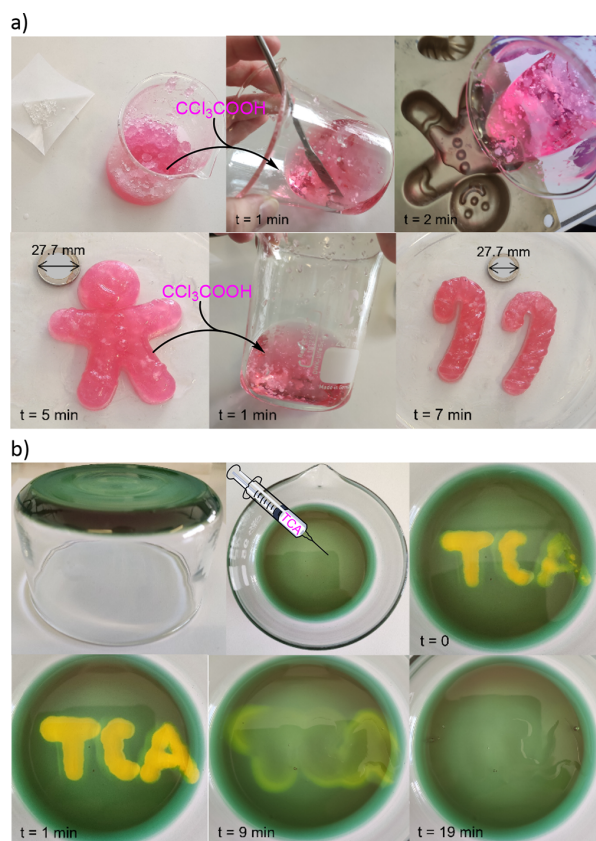
Figure 5. (a) Reusable gel to create several successive objects through gel−sol−gel transition. From a 60 mL DMF gel (5.38 mmol of **1**), successive additions of 8.59 mmol of TCA enable the triggering of gel−sol−gel cycles and molding of different objects. (b) Application of the gel−sol−gel process for a disappearing ink. From 15 mL of acidity-dependent colored indicator/DMF gel (0.948 mmol of **1**), writing was performed using a syringe containing a TCA solution (C = 0.65 mg/mL).

and green. Upon TCA decarboxylation, the green gel was regenerated and the message disappeared. This operation can be repeated several times. However, to reobtain a totally smooth surface, after two writing/self-erasing cycles, the gel was regenerated through a gel−sol−gel cycle by adding a larger amount of TCA.

Finally, the temporal control obtained through TCA addition was advantageously applied to generate new types of electrical systems. Supramolecular gels have recently been applied with success in the generation of new types of alternative flexible electrical systems.[63] Given their unique properties, they could find applications as self-healing, stretchable electrical systems[64−69] or in modulating electrical transport properties.[70]

In a complementary approach, we wondered about applying the TCA-fueled reversible gelation processes to create new types of reusable and flexible time-dependent electrical junctions (Figure 6; see the Supporting Information for details). To proceed, we designed an electrical system consisting of two parallel LEDS (one green (1) and one blue (2)), each of them connected to independent vials (1 and 2). On a 0.5 cm length junction (1 mL of DMF), both the DMF gel and TCA solution are conducting electricity.
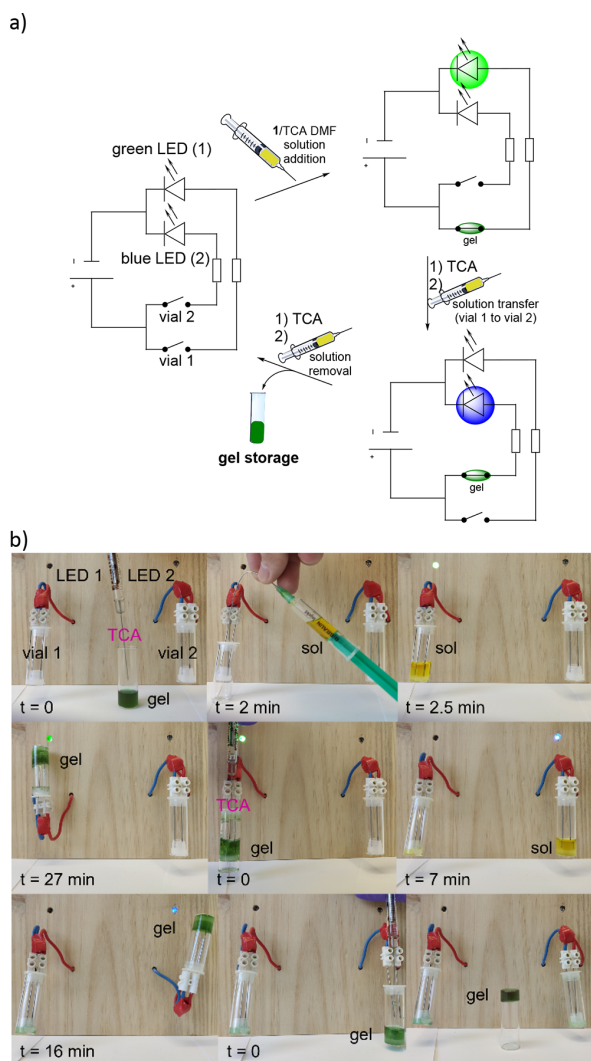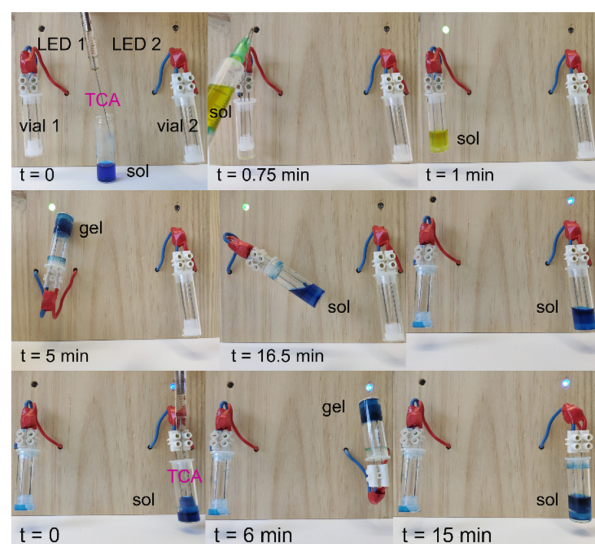

Figure 6. TCA-fueled electrical system based on a gel−sol−gel cycle. (a) Electrical system scheme used. From 1 mL of acidity-dependent colored indicator/DMF solution (0.12 mmol of **1**), gel−sol−gel cycles were performed by the addition of TCA solutions (80 μL, C = 0.65 mg/mL). The corresponding **1**.TCA DMF solution was transferred from one vial to another using a syringe. (b) Images of the electrical system obtained through successive gel−sol−gel cycles.

At first, to perform a reusable electrical junction, TCA was added on a previously formed gel (30 mg **1**, 1 mL DMF), and the resulting yellow solution was injected inside vial 1. Due to the conductivity of the solution, the green LED (1) lit up. Then after time-dependent decarboxylation, a strong green gel formed, generating a physically stable electrical junction. Next, the electrical junction was recycled by adding TCA and injecting the resulting solution inside vial 2 connected to the blue LED. After 16 min, a new strong gel was generated corresponding to the new electrical junction. This electrical junction could once again be recycled through the addition of TCA and stored in a vial under the gel form.

Overall, even though all compounds are rather cheap, the recyclability of an electrical junction is interesting in the context of more sustainable electrical systems. This new approach is also of potential interest to create temporary

flexible electrical junctions using syringes in poorly accessible locations where it is traditionally more challenging.

In a complementary application, these electrical systems could also be performed with temporal control through the application of a DBU-initiated sol−gel−sol switch (Figure 7).


Figure 7. TCA-fueled electrical system based on a sol−gel−sol cycle. From 1 mL of acidity-dependent colored indicator/DMF solution (0.12 mmol of **1** and 0.15 mmol of DBU), sol−gel−sol cycles were performed by the addition of TCA solutions (120 μL, C = 0.65 mg/mL). The corresponding **1**.DBU DMF solution was transferred from one vial to another using a syringe.

In this system, DBU is responsible for the formation of a solution at the resting state through the stabilization of an anionic form of the amino acid.[53] This is highly complementary and could enable the temporary formation of a strong gel, providing a flexible electrical system over a short period of time.

The electrical setup previously used has therefore been reused in the framework of a time-controlled electrical junction. Starting from a solution consisting of **1** and DBU in DMF, the addition of TCA induces the formation of an ammonium ion and allows the initiation of the first sol−gel−sol cycle in vial 1 where the green LED is switched on. As a consequence, a temporary strong electrical junction is generated through the gel formation before going back to a solution. This solution is then recycled by transferring it to vial 2, switching on the blue LED. Through another addition of TCA, a second sol−gel−sol cycle generates a temporary strong junction before once again going back to a solution that can be subsequently reused to create other electrical junctions.

Finally, the difference of conductivity between a TCA solution in DMF and the resulting neutral gel generated upon decarboxylation has been applied to create an electrical resistance with temporal control (Figure 8). This is possible if the length of the electrical junction is sufficient to block the electric current. To do so, a **1**.TCA solution in DMF was deposited to create a 20 cm connectivity between the wires. The current obtained through this junction is of 20 μA and enables the lighting of the green LED. Upon gel formation, resistance increases and the current drops to 2.4 μA, shutting
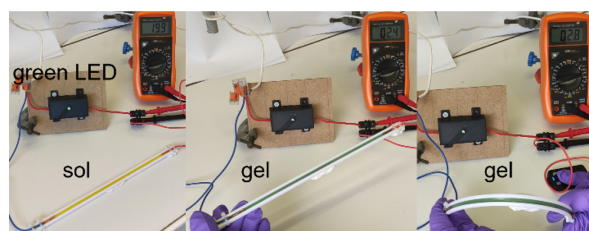
Figure 8. Electrical resistance with temporal control. Increase of the resistivity from left to right through the transition from a solution to a gel through an electrical junction initially made from acidity-dependent colored indicator 2 mL of the DMF solution, 0.08 mmol **1**, and 0.32 mmol TCA.

down the green light. Interestingly, when stretching the gel, a small increase in current (Δ = 0.7 μA) is observed, probably through an increase of the mobility of the solvent inside the gel matrix. This indicates that such systems can be further designed to obtain a response to a mechanical stress. Finally, the gel can be recycled from the junction for reuse in another system (Figure S28). It is important to highlight that given the time dependence of the gelation over the amount of TCA added, such system could enable to delay at will the apparition of electric resistance in an electrical system.

CONCLUSIONS

To conclude, TCA-fueled amine gelation enables to switch reversibly with time between solution and gel states. The systems are resilient, and at least 15 gel−sol−gel cycles could be performed with equal efficiency following TCA additions and subsequent decarboxylation to CO_2 and chloroform. We have shown that different amines and solvents could be applied, providing materials of different aspects and properties from strong gels to weaker ones.

The new materials generated are of great interest for a broad range of applications. For example, when applying chiral O-tert-butyl-ʟ-tyrosine, the gel−sol−gel transition induced chiroptical switching properties (−, +, −). The ability to reversibly switch between gel and solution upon TCA addition was also applied to mold successively different objects. Most interestingly, through the two complementary TCA-fueled gel−sol−gel and sol−gel−sol processes, new types of flexible and reusable electrical systems have been developed enabling transient electrical junctions or resistance between two wires. Such reusable flexible temporary electrical junctions should open broad perspectives for the design of electrical systems of improved complexity and functions.

The obtained properties using such simple systems are really inspiring and should find other applications in the near future for the design of innovative systems requiring reusability and temporal control.

METHODS

Reagents. All compounds were bought from Aldrich: trichloroacetic acid (BioXtra >99% quality), O-tert-butyl-ʟ-tyrosine (97% quality), and DBU (98% quality). O-tert-Butyl-ʟ-tyrosine (97% quality) bought from TCI was also tested and provided the same results. DMF and DMSO of anhydrous solvent quality were bought from Aldrich. Given the slow decomposition of TCA in DMF, TCA solutions were freshly prepared and used within 2 h.

Gel−Sol−Gel Cycles with O-tert-Butyl-ʟ-Tyrosine as Organogelator (Vial Inversion Method). A 4 mL vial was charged with 10 mg of O-tert-butyl-ʟ-tyrosine (0.0420 mmol), and 1 mL of DMF

was added, leading to a low solubilization of the amino acid. Then 40 μL of the TCA/DMF solution (C = 0.65 mg/μL, 0.159 mmol) was added, and the solution was shaken, resulting in the solubilization of *O-tert*-butyl-L-tyrosine. After 3−4 min at RT (30 °C), a strong gel was formed, and the vial was set upside down. The gel−sol−gel system can also be monitored as previously reported using the BTB/BPB (C = 0.05/0.18 mg/mL) DMF solution. Gels were stable for several months.

O-tert-Butyl-L-Tyrosine Gel−Sol−Gel Kinetic by UV Absorption. Gel−sol−gel spectra were recorded on a JASCO V-670 spectrometer equipped with a JASCO Peltier cell holder ETCS-761 to maintain the temperature at 20.0 °C. A 1 cm quartz cuvette was charged with 10 mg of *O-tert*-butyl-L-tyrosine (0.042 mmol), and then 2 mL of DMF was added, leading to a low solubilization. Then 40 μL of the TCA/DMF solution (0.65 mg/μL, 0.159 mmol) was added, and the solution was shaken, resulting in the solubilization of *O-tert*-butyl-L-tyrosine. After a few minutes, a strong gel was formed. Then one gel−sol−gel cycle was performed by adding the TCA/DMF solution (0.65 mg/μL) to the gel. The solution was quickly mixed three times with a syringe, and the absorbance was measured.

Rheology Measure over Two Successive TCA Additions Using _O-tert_-Butyl-L-Tyrosine. Dynamic viscoelastic properties were determined with a controlled-stress rheometer (CR 302 of Anton Paar) using an aluminum plate/plate geometry (diameter 25 mm). The applied strain during the dynamical measurements for time sweep was settled at 5%. The temperature was controlled (±3 °C) at 25 °C. *O-tert*-Butyl-L-tyrosine (0.075 mmol) was placed in 2 mL of DMF in a small vial (the amino acid is poorly soluble). Trichloroacetic acid (0.46 mmol) was then added, and the vial was closed and shaken during 30 s to solubilize the *O-tert*-butyl-L-tyrosine. Five hundred microliters of the obtained solution was taken from the vial with a syringe, and 300 μL of this solution was placed in the rheometer with a gap of 500 μm. The measurement of the solution to gel first cycle started 9 min after the addition of TCA. With the TCA consumption, the gel formation was clearly observed. When a strong gel was formed according to the high and stable storage and loss modulus, 0.33 mmol of trichloroacetic acid was added again to the gel in the vial, and the vial was closed and shaken during 30 s, resulting in the formation of a solution. Three hundred microliters of this solution was placed in the rheometer with a gap of 500 μm, and the measurement of the solution to gel second cycle immediately started. With the TCA consumption, the gel formation was clearly observed, leading to the same loss and storage modulus as during the first cycle.

Electronic Circular Dichroism. Electronic circular dichroism (ECD) coupled with UV−vis spectra was measured on a JASCO J-815 spectrometer equipped with a JASCO Peltier cell holder PTC-423 to maintain the temperature at 20.0 °C. A vial was charged with *O-tert*-butyl-L-tyrosine (10.0 mg, 0.042 mmol) and then 2 mL of DMF, leading to a low solubilization of the *O-tert*-butyl-L-tyrosine. Then 40 μL of a TCA/DMF solution (C = 0.65 mg/μL, 0.159 mmol) was added, and the solution was shaken for 30 s, resulting in the total solubilization of *O-tert*-butyl-L-tyrosine. Finally, 300 μL of this solution was transferred into a quartz cell of 2 mm optical path. Gel−sol−sol cycles were performed by the addition of 4.5 μL of the TCA solution (C = 0.65 mg/μL, 0.0179 mmol) inside the cuvette. Upon TCA addition, the solution was quickly mixed five times with a syringe. Fifteen consecutives cycles were performed.

Gel−Sol−Gel Cycles by the Vial Inversion Method Using _O-tert_-Octadecylamine. A 4 mL vial was charged with 40 mg of octadecylamine (0.148 mmol), and then 1 mL of DMSO was added, leading to a low solubilization of the amine. Sol−gel−sol cycles were then repeated by successive additions of solid TCA (45 ± 10 mg), and the vial was closed and shaken during 20 s before standing for 3 ± 1 min, at which point a strong gel was formed as confirmed by vial inversion. After 12 cycles, the gel was not strong enough for vial inversion.

Writing and Self-Erasing. To a 250 mL large beaker were added 225 mg of *O-tert*-butyl-L-tyrosine (0.948 mmol) and 15 mL of the BTB/BPB DMF solution. TCA (300 mg, 1.84 mmol) was then added. The solution was mixed (gentle beaker shaking) for 1.5 min.

After 5−10 min, a strong and resistant green gel was formed. Writing on the gel surface was performed by adding drops of the TCA solution (C = 0.65 mg/mL, 50 to 100 μL). At the location of the drops, a yellow liquid was generated, while the gel not in contact with TCA remained resistant and green. After 15−19 min, the uniform green gel was generated back again. Writing and self-erasing can be performed again through another writing through the addition of drops of the TCA solution (C = 0.65 mg/mL, 50 to 100 μL).

Successive Object Molding. To a 250 mL beaker were added 1.28 g of *O-tert*-butyl-L-tyrosine (5.38 mmol, 1.00 equiv) and 60 mL of DMF followed by 1.40 g of TCA (8.59 mmol, 1.60 equiv). The solution was mixed (gentle beaker shaking) for 1.5 min. After 5−10 min, a strong gel was formed and used to perform the subsequent moldings. To perform molding through gel−sol−gel cycles, this gel was mixed with a spatula and then 1.40 g of TCA (8.59 mmol, 1.60 equiv) was added. The obtained solution was mixed (gentle beaker shaking) for 1.5 min and poured inside the mold to form a gel after 6 ± 1 min. The silicone mold used is a typical mold used for cake baking. The gel can then be removed from the mold. Subsequent gel−sol−gel cycles can be performed by mixing the gel with a spatula and then adding 1.40 g of TCA (8.59 mmol, 1.60 equiv). Four molding cycles were performed: three "Gingerbread man" gels (60 mL) and one "candy cane" gel (2 × 30 mL). After the last molding, the "Gingerbread man" gel was allowed to disappear in the TCA/DMF solution (15 g TCA/10 mL DMF). After standing for 72 h, a strong gel was formed again.

Electric Systems Based on TCA as Fuel. The generator used delivered 9.18 V and 23 mA to the complete system. The resistance value was 220 Ω. The vial used has a diameter of 1.3 cm and is 4.5 cm tall. Needles (Braun Sterican, Ø 0.80 × 120 mm) were used as conductor. LEDs used were as follows: 5 mm blue LED (I/VF: 20 mA/3−3.2 V, LI 7000−8000 mcd) and 5 mm green LED (I/VF: 20 mA/3−3.2 V, LI 15,000−18,000 mcd). The system used consists of two parallel vials, each one connected to a different LED.

Gel−Sol−Gel System. The gel−sol−gel system was prepared with *O-tert*-butyl-L-tyrosine (30 mg) and 1 mL of the BTB/BPB DMF solution. A first initiation gel−sol−gel was performed with 80 μL of the TCA/DMF solution (0.65 mg/μL). A gel−sol−gel cycle was then started by the addition of 80 μL of the TCA/DMF solution (0.65 mg/μL). The resulting solution was transferred inside the "green LED switch" followed by light emission from the green LED. After the gel formation, the vial was set upside down and shaken without any gel destruction or loss in green light intensity. A second gel−sol−gel cycle was then started by adding 60 μL of the TCA/DMF solution (0.65 mg/μL). After the gel dissolution, the resulting solution was transferred into the "blue LED switch" vial followed by light emission from the blue LED. Then after the gel formation, the vial was set upside down and shaken without any gel destruction or loss in blue light intensity. Finally, a third gel−sol−gel cycle was then started by adding 80 μL of the TCA/DMF solution (0.65 mg/μL). After the gel dissolution, the resulting solution was transferred into the original vial for storage.

Sol−Gel−Sol System. The sol−gel−sol system was prepared with *O-tert*-butyl-L-tyrosine (30 mg), DBU (24 mg), and 1 mL of the BTB/BPB DMF solution. Then a first initiation sol−gel−sol was performed with 150 μL of the TCA/DMF solution (0.65 mg/μL). A sol−gel−sol cycle was then started with the addition of 150 μL of the TCA/DMF solution (0.65 mg/μL). The resulting solution was transferred inside the "green LED switch" followed by light emission from the green LED. After the gel formation, the vial was set upside down and shaken without any gel destruction or loss in green light intensity. After the gel dissolution, the resulting solution was transferred into the "blue LED switch" vial followed by light emission from the blue LED. A second sol−gel−sol cycle was then started with the addition of 150 μL of the TCA/DMF solution (0.65 mg/μL). Then after the gel formation, the vial was set upside down and shaken without any gel destruction or loss in blue light intensity. After the gel dissolution, the resulting solution was transferred into the original vial.

■ AUTHOR INFORMATION

Corresponding Author

    Adrien Quintard − *Aix Marseille Univ, CNRS, Centrale Marseille, iSm2, 13397 Marseille, France;* ⓘ orcid.org/ 0000-0003-0193-6524; Email: adrien.quintard@univ-amu.fr

Authors

    Enzo Olivieri − *Aix Marseille Univ, CNRS, Centrale Marseille, iSm2, 13397 Marseille, France*

    Baptiste Gasch − *Aix Marseille Univ, CNRS, Centrale Marseille, iSm2, 13397 Marseille, France*

    Guilhem Quintard − *Université de Lyon, INSA LYON, Ingénierie des Matériaux Polymères IMP-UMR CNRS 5223, F 69621 Villeurbanne, France*

    Jean-Valère Naubron − *Aix Marseille Univ, CNRS, Centrale Marseille, Spectropole, FR1739 Marseille, France;* ⓘ orcid.org/0000-0002-8523-4476

■ REFERENCES

(1) Das, K.; Gabrielli, L.; Prins, L. J. Chemically Fueled Self-Assembly in Biology and Chemistry. *Angew. Chem., Int. Ed.* **2021**, *60*, 20120−20143.

(2) van Rossum, S. A. P.; Tena-Solsona, M.; van Esch, J. H.; Eelkema, R.; Boekhoven, J. Dissipative Out-of-Equilibrium Assembly of Man-made Supramolecular Materials. *Chem. Soc. Rev.* **2017**, *46*, 5519−5535.

(3) De, S.; Klajn, R. Dissipative Self-Assembly Driven by the Consumption of Chemical Fuels. *Adv. Mater.* **2018**, *30*, 1706750.

(4) Singh, N.; Formon, G. J. M.; De Piccoli, S.; Hermans, T. M. Devising Synthetic Reaction Cycles for Dissipative Nonequilibrium Self-Assembly. *Adv. Mater.* **2020**, *32*, 1906834.

(5) Wang, G.; Liu, S. Strategies to Construct a Chemical-Fuel-Driven Self-Assembly. *ChemSystemsChem* **2020**, *2*, No. e1900046.

(6) Leng, Z. J.; Peng, F.; Hao, X. Chemical-Fuel-Driven Assembly in Macromolecular Science: Recent Advances and Challenges. *ChemPlusChem* **2020**, *85*, 1190−1199.

(7) Rieß, B.; Grötsch, K. R.; Boekhoven, J. The Design of Dissipative Molecular Assemblies Driven by Chemical Reaction Cycles. *Chem* **2020**, *6*, 552−578.

(8) Panja, S.; Adams, D. J. Stimuli Responsive Dynamic Transformations in Supramolecular Gels. *Chem. Soc. Rev.* **2021**, *50*, 5165.

(9) Rieß, B.; Boekhoven, J. Applications of Dissipative Supramolecular Materials with a Tunable Lifetime. *ChemNanoMat* **2018**, *4*, 710−719.

(10) Boekhoven, J.; Brizard, A. M.; Kowlgi, K. N. K.; Koper, G. J. M.; Eelkema, R.; van Esch, J. H. Dissipative Self-Assembly of a Molecular Gelator by using a Chemical Fuel. *Angew. Chem., Int. Ed.* **2010**, *49*, 4825−4828.

(11) Boekhoven, J.; Hendriksen, W. E.; Koper, G. J. M.; Eelkema, R.; van Esch, J. H. Transient Assembly of Active Materials Fueled by a Chemical Reaction. *Science* **2015**, *349*, 1075−1079.

(12) Tena-Solsona, M.; Rieβ, B.; Grötsch, R. K.; Löhrer, F. C.; Wanzke, C.; Käsdorf, B.; Bausch, A. R.; Müller-Buschbaum, P.; Lieleg, O.; Boekhoven, J. Non-equilibrium Dissipative Supramolecular Materials with a Tunable Lifetime. *Nat. Commun.* **2017**, *8*, 15895−15903.

(13) Bal, S.; Das, K.; Ahmed, S.; Das, D. Chemically Fueled Dissipative Self-Assembly that Exploits Cooperative Catalysis. *Angew. Chem., Int. Ed.* **2019**, *58*, 244−247.

(14) Afrose, S. P.; Bal, S.; Chatterjee, A.; Das, K.; Das, D. Designed Negative Feedback from Transiently Formed Catalytic Nanostructures. *Angew. Chem., Int. Ed.* **2019**, *58*, 15783−15787.

(15) Zhang, B.; Jayalath, I. M.; Ke, J.; Sparks, J. L.; Hartley, C. S.; Konkolewicz, D. Chemically Fueled Covalent Crosslinking of Polymer Materials. *Chem. Commun.* **2019**, *55*, 2086−2089.

(16) Dai, K.; Fores, J. R.; Wanzke, C.; Winkeljann, B.; Bergmann, A. M.; Lieleg, O.; Boekhoven, J. Regulating Chemically Fueled Peptide Assemblies by Molecular Design. *J. Am. Chem. Soc.* **2020**, *142*, 14142−14149.

(17) Wojciechowski, J. P.; Martin, A. D.; Thordarson, P. Kinetically Controlled Lifetimes in Redox-Responsive Transient Supramolecular Hydrogels. *J. Am. Chem. Soc.* **2018**, *140*, 2869−2874.

(18) Ogden, W. A.; Guan, Z. Redox Chemical-Fueled Dissipative Self-Assembly of Active Materials. *ChemSystemsChem* **2020**, *2*, No. e1900030.

(19) Debnath, S.; Roy, S.; Ulijn, R. V. Peptide Nanofibers with Dynamic Instability through Nonequilibrium Biocatalytic Assembly. *J. Am. Chem. Soc.* **2013**, *135*, 16789−16792.

(20) Pezzato, C.; Prins, L. J. Transient Signal Generation in a Self-Assembled Nanosystem Fueled by ATP. *Nat. Commun.* **2015**, *6*, 7790−7797.

(21) Heuser, T.; Weyandt, E.; Walther, A. Biocatalytic Feedback-Driven Temporal Programming of Self-Regulating Peptide Hydrogels. *Angew. Chem., Int. Ed.* **2015**, *54*, 13258−13262.

(22) Angulo-Pachón, C. A.; Miravet, J. F. Sucrose-Fueled, Energy Dissipative, Transient Formation of Molecular Hydrogels mediated by Yeast Activity. *Chem. Commun.* **2016**, *52*, 5398−5401.

(23) Maiti, S.; Fortunati, I.; Ferrante, C.; Scrimin, P.; Prins, L. J. Dissipative Self-Assembly of Vesicular Nanoreactors. *Nat. Chem.* **2016**, *8*, 725−731.

(24) Sahoo, J. K.; Pappas, C. G.; Sasselli, I. R.; Abul-Haija, Y. M.; Ulijn, R. V. Biocatalytic Self-Assembly Cascades. *Angew. Chem., Int. Ed.* **2017**, *56*, 6828−6832.

(25) Heinen, L.; Heuser, T.; Steinschulte, A.; Walther, A. Antagonistic Enzymes in a Biocatalytic pH Feedback System Program

Autonomous DNA Hydrogel Life Cycles. *Nano Lett.* **2017**, *17*, 4989−4995.

(26) Che, H.; Buddingh', B. C.; van Hest, J. C. M. Self-Regulated and Temporal Control of a "Breathing" Microgel Mediated by Enzymatic Reaction. *Angew. Chem., Int. Ed.* **2017**, *56*, 12581−12585.

(27) Hao, X.; Sang, W.; Hu, J.; Yan, Q. Pulsating Polymer Micelles via ATP-Fueled Dissipative Self-Assembly. *ACS Macro Lett.* **2017**, *6*, 1151−1155.

(28) Mondal, S.; Podder, D.; Nandi, S. K.; Chowdhury, S. R.; Haldar, D. Acid-Responsive Fibrillation and Urease-Assisted Defibrillation of Phenylalanine: a Transient Supramolecular Hydrogel. *Soft Matter* **2020**, 10115−10121.

(29) Zhong, Y.; Li, P.; Hao, J.; Wang, X. Bioinspired Self-Healing of Kinetically Inert Hydrogels Mediated by Chemical Nutrient Supply. *ACS Appl. Mater. Interfaces* **2020**, *12*, 6471−6478.

(30) Postma, S. G. J.; Vialshin, I. N.; Gerritsen, C. Y.; Bao, M.; Huck, W. T. S. Preprogramming Complex Hydrogel Responses using Enzymatic Reaction Networks. *Angew. Chem., Int. Ed.* **2017**, *56*, 1794−1798.

(31) Panja, S.; Adams, D. J. Gel to Gel Transitions by Dynamic Self-Assembly. *Chem. Commun.* **2019**, *55*, 10154−10157.

(32) Hu, K.; Sheiko, S. S. Time Programmable Hydrogels: Regulating the Onset Time of Network Dissociation by a Reaction Relay. *Chem. Commun.* **2018**, *54*, 5899−5902.

(33) Singh, N.; Lainer, B.; Formon, G. J. M.; De Piccoli, S.; Hermans, T. M. Re-Programming Hydrogel Properties Using a Fuel-Driven Reaction Cycle. *J. Am. Chem. Soc.* **2020**, *142*, 4083−4087.

(34) Panja, S.; Fuentes-Caparrós, A. M.; Cross, E. R.; Cavalcanti, L.; Adams, D. J. Annealing Supramolecular Gels by a Reaction Relay. *Chem. Mater.* **2020**, *32*, 5264−5271.

(35) Dhiman, S.; Jalani, K.; George, S. J. Redox-Mediated, Transient Supramolecular Charge-Transfer Gel and Ink. *ACS Appl. Mater. Interfaces* **2020**, *12*, 5259−5264.

(36) Gao, Z.; Qiu, S.; Yan, F.; Zhang, S.; Wang, F.; Tian, W. Time-encoded Bio-Fluorochromic Supramolecular Co-Assembly for Re-writable Security Printing. *Chem. Sci.* **2021**, *12*, 10041−10047.

(37) Wood, C. S.; Browne, C.; Wood, D. M.; Nitschke, J. R. Fuel-Controlled Reassembly of Metal−Organic Architectures. *ACS Cent. Sci.* **2015**, *1*, 504−509.

(38) Jia, L.; Kilbey, S. M., II; Wang, X. Tailoring Azlactone-Based Block Copolymers for Stimuli-Responsive Disassembly of Nano-carriers. *Langmuir* **2020**, *36*, 10200−10209.

(39) Go, D.; Rommel, D.; Liao, Y.; Haraszti, T.; Sprakel, J.; Kuehne, A. J. C. Dissipative Disassembly of Colloidal Microgel Crystals Driven by a Coupled Cyclic Reaction Network. *Soft Matter* **2018**, *14*, 910−915.

(40) Abe, Y.; Okamura, H.; Nakazono, K.; Koyama, Y.; Uchida, S.; Takata, T. Thermoresponsive Shuttling of Rotaxane Containing Trichloroacetate Ion. *Org. Lett.* **2012**, *14*, 4122−4125.

(41) Zhu, N.; Nakazono, K.; Takata, T. Solid-state Rotaxane Switch: Synthesis of Thermoresponsive Rotaxane Shuttle Utilizing a Thermally Decomposable Acid. *Chem. Lett.* **2016**, *45*, 445−447.

(42) Erbas-Cakmak, S.; Fielden, S. D. P.; Karaca, U.; Leigh, D. A.; McTernan, C. T.; Tetlow, D. J.; Wilson, M. R. Rotary and Linear Molecular Motors Driven by Pulses of a Chemical Fuel. *Science* **2017**, *358*, 340−343.

(43) Biagini, C.; Fielden, S. D. P.; Leigh, D. A.; Schaufelberger, F.; Di Stefano, S.; Thomas, D. Dissipative Catalysis with a Molecular Machine. *Angew. Chem., Int. Ed.* **2019**, *58*, 9876−9880.

(44) Choi, S.; Mukhopadhyay, R. D.; Kim, Y.; Hwang, I.-C.; Hwang, W.; Ghosh, S. K.; Baek, K.; Kim, K. Fuel-Driven Transient Crystallization of a Cucurbit[8]uril-Based Host−Guest Complex. *Angew. Chem., Int. Ed.* **2019**, *58*, 16850−16853.

(45) Thomas, A.; Gasch, B.; Olivieri, E.; Quintard, A. Trichloroacetic Acid Fueled Practical Amine Purifications. *Beilstein J. Org. Chem.* **2022**, *18*, 225−231.

(46) Biagini, C.; Di Stefano, S. Abiotic Chemical Fuels for the Operation of Molecular Machines. *Angew. Chem., Int. Ed.* **2020**, *59*, 8344−8354.

(47) Berrocal, J. A.; Biagini, C.; Mandolini, L.; Di Stefano, S. Coupling of the Decarboxylation of 2-Cyano-2-phenylpropanoic Acid to Large-Amplitude Motions: A Convenient Fuel for an Acid-Base-Operated Molecular Switch. *Angew. Chem., Int. Ed.* **2016**, *55*, 6997−7001.

(48) Ghosh, A.; Paul, I.; Adlung, M.; Wickleder, C.; Schmittel, M. Oscillating Emission of [2]Rotaxane Driven by Chemical Fuel. *Org. Lett.* **2018**, *20*, 1046−1049.

(49) Ghosh, A.; Paul, I.; Schmittel, M. Multitasking with Chemical Fuel: Dissipative Formation of a Pseudorotaxane Rotor from Five Distinct Components. *J. Am. Chem. Soc.* **2021**, *143*, 5319−5323.

(50) Del Giudice, D.; Spatola, E.; Valentini, M.; Bombelli, C.; Ercolani, G.; Di Stefano, S. Time-Programmable pH: Decarboxylation of Nitroacetic Acid allows the Time-Controlled Rising of pH to a Definite Value. *Chem. Sci.* **2021**, *12*, 7460−7466.

(51) Goswami, A.; Saha, S.; Elramadi, E.; Ghosh, A.; Schmittel, M. Off-Equilibrium Speed Control of a Multistage Molecular Rotor: 2-Fold Chemical Fueling by Acid or Silver(I). *J. Am. Chem. Soc.* **2021**, *143*, 14926−14935.

(52) Mariottini, D.; Del Giudice, D.; Ercolani, G.; Di Stefano, S.; Ricci, F. Dissipative Operation of pH-Responsive DNA-Based Nanodevices. *Chem. Sci.* **2021**, *12*, 11735−11739.

(53) Olivieri, E.; Quintard, G.; Naubron, J.-V.; Quintard, A. Chemically Fueled Three-State Chiroptical Switching Supramolecular Gel with Temporal Control. *J. Am. Chem. Soc.* **2021**, *143*, 12650−12657.

(54) See ref 53 and: Aykent, G.; Zeytun, C.; Marion, A.; Özçubukçcu, S. Simple Tyrosine Derivatives Act as Low Molecular Weight Organogelators. *Sci. Rep.* **2019**, *9*, 4893−4900.

(55) George, M.; Weiss, R. G. Chemically Reversible Organogels: Aliphatic Amines as "Latent" Gelators with Carbon Dioxide. *J. Am. Chem. Soc.* **2001**, *123*, 10393−10394.

(56) George, M.; Weiss, R. G. Chemically Reversible Organogels via "Latent" Gelators. Aliphatic Amines with Carbon Dioxide and Their Ammonium Carbamates. *Langmuir* **2002**, *18*, 7124−7135.

(57) Clelland, C. T.; Risca, V.; Bancroft, C. Hiding Messages in DNA Microdots. *Nature* **1999**, *399*, 533−534.

(58) Feringa, B. L.; van Delden, R. A.; Koumura, N.; Geertsema, E. M. Chiroptical Molecular Switches. *Chem. Rev.* **2000**, *100*, 1789−1816.

(59) Brandt, J. R.; Salerno, F.; Fuchter, M. J. The Added Value of Small-Molecule Chirality in Technological Applications. *Nat. Rev.* **2017**, *1*, No. 0045.

(60) Erbas-Cakmak, S.; Kolemen, S.; Sedgwick, A. C.; Gunnlaugsson, T.; James, T. D.; Yoon, J.; Akkaya, E. U. Molecular Logic Gates: the Past, Present and Future. *Chem. Soc. Rev.* **2018**, *47*, 2228−2248.

(61) Zhang, L.; Wang, H.-X.; Li, S.; Liu, M. Supramolecular Chiroptical Switches. *Chem. Soc. Rev.* **2020**, *49*, 9095−9120.

(62) Colquhoun, H.; Lutz, J.-F. Information-Containing Macro-molecules. *Nat. Chem.* **2014**, *6*, 455−456.

(63) For a review, see: Deng, Z.; Wang, H.; Mac, P. X.; Guo, B. Self-Healing Conductive Hydrogels: Preparation, Properties and Applications. *Nanoscale* **2020**, *12*, 1224−1246.

(64) Shi, Y.; Wang, M.; Ma, C.; Wang, Y.; Li, X.; Yu, G. A Conductive Self-Healing Hybrid Gel Enabled by Metal−Ligand Supramolecule and Nanostructured Conductive Polymer. *Nano Lett.* **2015**, *15*, 6276−6281.

(65) Lee, Y.-Y.; Kang, H.-Y.; Gwon, S. H.; Choi, G. M.; Lim, S.-M.; Sun, J.-Y.; Joo, Y.-C. A Strain-Insensitive Stretchable Electronic Conductor: PEDOT:PSS/Acrylamide Organogels. *Adv. Mater.* **2016**, *28*, 1636−1643.

(66) Lee, H.; Ha, Y.-M.; Lee, S. H.; Ko, Y.-I.; Muramatsu, H.; Kim, Y. A.; Park, M.; Jung, Y. C. Spontaneously Restored Electrical Conductivity of Bioactive Gel Comprising Mussel Adhesive Protein-coated Carbon Nanotubes. *RSC Adv.* **2016**, *6*, 87044−87048.

(67) Han, L.; Lu, X.; Wang, M.; Gan, D.; Deng, W.; Wang, K.; Fang, L.; Liu, K.; Chan, C. W.; Tang, Y.; Weng, L.-T.; Yuan, H. A Mussel-Inspired Conductive, Self-Adhesive, and Self-Healable Tough Hydro-

gel as Cell Stimulators and Implantable Bioelectronics. *Small* **2017**, *13*, 1601916.

(68) Darabi, M. A.; Khosrozadeh, A.; Mbeleck, R.; Liu, Y.; Chang, Q.; Jiang, J.; Cai, J.; Wang, Q.; Luo, G.; Xing, M. Skin-Inspired Multifunctional Autonomic-Intrinsic Conductive Self-Healing Hydrogels with Pressure Sensitivity, Stretchability, and 3D Printability. *Adv. Mater.* **2017**, *29*, 1700533.

(69) Park, J.; Kim, K. Y.; Kim, C.; Lee, J. H.; Kim, J. H.; Lee, S. S.; Choi, Y.; Jung, J. H. A crown-Ether-Based Moldable Supramolecular Gel with Unusual Mechanical Properties and Controllable Electrical Conductivity Prepared by Cation-Mediated Cross-Linking. *Polym. Chem.* **2018**, *9*, 3900−3907.

(70) Bal, S.; Ghosh, C.; Ghosh, T.; Vijayaraghavan, R. K.; Das, D. Non-Equilibrium Polymerization of Cross-β Amyloid Peptides for Temporal Control of Electronic Properties. *Angew. Chem., Int. Ed.* **2020**, *59*, 13506−13510.